Rev. Adv. Mater. Sci. 51 (2017) 130-148

ELASTIC MODELS OF DEFECTS IN 3D AND 2D CRYSTALS

A.L. Kolesnikova[1,2], M.Yu. Gutkin[1,2,3] and A.E. Romanov[1,4]

[1]ITMO University, Kronverkskiy pr. 49, Saint Petersburg, 197101, Russia
[2]Institute of Problems of Mechanical Engineering, Russian Academy of Sciences, Bolshoj pr. 61, V.O., Saint Petersburg, 199178, Russia
[3]Peter the Great St.Petersburg Polytechnic University, Polytekhnicheskaya 29, Saint Petersburg, 195251, Russia
[4]Ioffe Institute, Russian Academy of Sciences, Polytekhnicheskaya 26, Saint Petersburg, 194021, Russia

Received: April 24, 2017

Abstract. We present the elastic models of defects in crystals exploring the framework of continuum mechanics of solids. The key feature of the defects attributed to zero-, one-, two- or three-dimensional ones is the dimension of the region of their *eigenstrains*. It is shown how from the elastic fields of defects of a lower dimension to build, by integration, the elastic fields of defects of a higher dimension. On the base of the elastic fields of infinitesimal dislocation loops, the fields of the circular dilatation line, the circular dilatation disk, and the cylindrical and hemispherical inclusions are derived in a step-by-step manner. In the final part of the paper, the elastic fields of defects in 2D crystals are considered.

1. INTRODUCTION

The theory of defects of a continuous elastic medium, on the one hand, is a mathematical description of the elastic behavior of defects in solids, and on the other hand, it is a tool for modeling the elastoplastic behavior of materials experiencing local transformations due to mechanical or thermal treatments.

The theory of defects owes its modern appearance to the efforts of many scientists, beginning with Volterra [1], who first presented elastic models of dislocations and disclinations. The foundations of the theory were laid down in the fundamental studies by Eshelby [2-4], Kröner [3], Kroupa [5], Indenbom [6], De Wit [7], Hirth [8], Lothe [8], Teodosiu [9], Mura [10], and many others.

At different stages of the defect theory development, various aspects of it become important. Currently, topical problems include consideration of defects in finite solids and films that is directly related to physical and mechanical problems of nanoheterostructures, nanowires, nanoparticles, nanocomposites, and 2D crystals, such as graphene.

Nowadays it is known that for the solution of boundary-value problems it is effective to use the virtual defect technique, e.g. see Refs. [11-13]. This technique originates from the method of surface dislocations [14,15]. The technique operates with elastic fields of distributed virtual sources of elastic fields used to construct the boundary integral equations. Solving the equations with respect to the distribution functions of defects one finds the solution for the boundary-value elastic problem of the interest. Often it is not enough to have Volterra dislocations and disclinations as virtual defects, and it is necessary to introduce other types of virtual defects of various configurations, for example, the circular radial Somigliana dislocation [11,13,16,17]. In addi-

Corresponding author: A.E. Romanov, e-mail: aer@mail.ioffe.ru

tion, we believe that circular dilatation and shear lines will serve as convenient virtual defects for solving axisymmetric boundary-value problems. To find the solutions to more general problems, one can use dislocation half-loops [12], rays and infinitesimal dislocation loops [5].

The purpose of this paper is to provide a brief review of the latest achievements in elastic description of defects in 3D and 2D crystals. In the framework of the formal classification, based on dimension of region of defect's *eigenstrain*, it will be demonstrated how from the elastic fields of defects of a lower dimension to get, by integration, the elastic fields of defects of a higher dimension. As an example, a step-by-step path from an infinitesimal dislocation loop through a circular dilatation line and a circular dilatation disk to axisymmetric inclusions in the form of a finite circular cylinder and a hemisphere will be presented. The final part of the article shows the progress of recent years in the construction of elastic models of defects in 2D crystals.

2. CLASSIFICATION OF INTERNAL SOURCES OF ELASTIC FIELDS IN 3D CONTINUUM

Elastic fields in solids can be caused either by external forces applied to the boundaries of the body, or by internal sources presented in the body. Internal sources (or defects) distort the elastic medium, which is a crystal, and thereby generate elastic fields in it. We do not consider *eigestrain*-free inhomogeneities, i.e. regions with other elastic modules but with no *eigenstrains*, and voids as intrinsic defects. These inhomogeneities and voids themselves are not the sources of elastic fields, but they only distort the existing elastic fields.

In our opinion, there are three basic approaches for specifying the internal sources of elastic fields: (a) using the distribution of forces with or without a moment (see, for example, [18]), (b) using *eigenstrain* (see, for example, [2-4,10]), and (c) exploring harmonic stress-functions, which are the solutions of harmonic differential equations with prescribed source terms [9,16,17,19]. These approaches are used to build mathematical models of real physical defects in the crystal lattice, e.g. point defects, dislocations and inclusions. The basic principle in all the approaches is that the elastic fields of the defect under consideration satisfies the equilibrium equations for stresses.

The "force" approach (a) makes it possible to find the elastic fields of the defect using the volume force distributions [9,18]. This approach can be effectively applied to calculate the fields of point centers of dilatation, which in the real crystal lattice mimic vacancies or impurity atoms. In the case of dislocations, the force approach also works, although in a not so obvious way [20]. Direct and clear methods to defect modeling are the approaches exploring *eigenstrain* (b) and harmonic functions or displacements (c). In this paper, we work in the framework of the "*eigenstrain*" approach.

In micromechanics of elastic continuum, the concept of the *eigenstrain* tensor, which determines the way of specifying and region of localization of the defect, can be used to uniquely define any kind of defect. *Eigenstrain* is a complete characteristic of the defect. The response of an elastic medium to a given *eigenstrain* unambiguously determines the elastic fields of the defect in the medium. The mathematical apparatus for finding the elastic fields of the defect from a given *eigenstrain* is well developed [2-4,5,10].

The process of specifying *eigenstrain* can be presented in the way that was first proposed by Eshelby for inclusions [2]. The Eshelby procedure can be outlined as follows: a cut is made in an elastic body, the material is removed, and then it is plastically deformed. Forces are applied to this deformed volume of material in order to insert it into the original place exactly at the place of the cut, then, the surfaces of the cut are glued together and the forces are removed.

If we apply the Eshelby procedure to regions of different dimensions, we can obtain defects of different dimensions, and introduce a classification of defects in an elastic medium, based on the dimension n of the region Ω_n of *eigenstrain* ${}^{n}\varepsilon^{*}_{ij}$ (or *self-distortion* ${}^{n}\beta^{*}_{ij}$).

In 3D elastic space, defects can be subdivided into four classes.

***Zero-dimensional or point defects* (*n* = 0).** After Kroupa [5], we define infinitesimal dislocation loops as the elementary zero-dimensional defects (Figs. 1a and 1b). The self-distortion of an infinitesimal dislocation loop can be written as follows [21]:

$$ {}^{0}\beta^{*}_{ij} = -b_j s_i \delta(\mathbf{R} - \mathbf{R}_0), \quad i, j = x, y, z, \tag{1} $$

where b_j is Burgers vector of dislocation loop, placed in point $\mathbf{R}_0$, s_i is an area of the loop. The 3D Dirac delta-function $\delta(\mathbf{R}\text{-}\mathbf{R}_0)$ is defined by the product of the 1D delta-functions: $\delta(\mathbf{R}\text{-}\mathbf{R}_0)= \delta(x\text{-}x_0)\ \delta(y\text{-}y_0)\ \delta(z\text{-}z_0)$. It has the following dimensionality: $[\delta(\mathbf{R}\text{-}\mathbf{R}_0)]= [\delta(x\text{-}x_0)][\delta(y\text{-}y_0)][\delta(z\text{-}z_0)]=X^{-1}X^{-1}X^{-1}=X^{-3}$, where X is a unit of length. The distortion given by Eq. (1) can be defined for any orthogonal coordinate system, for

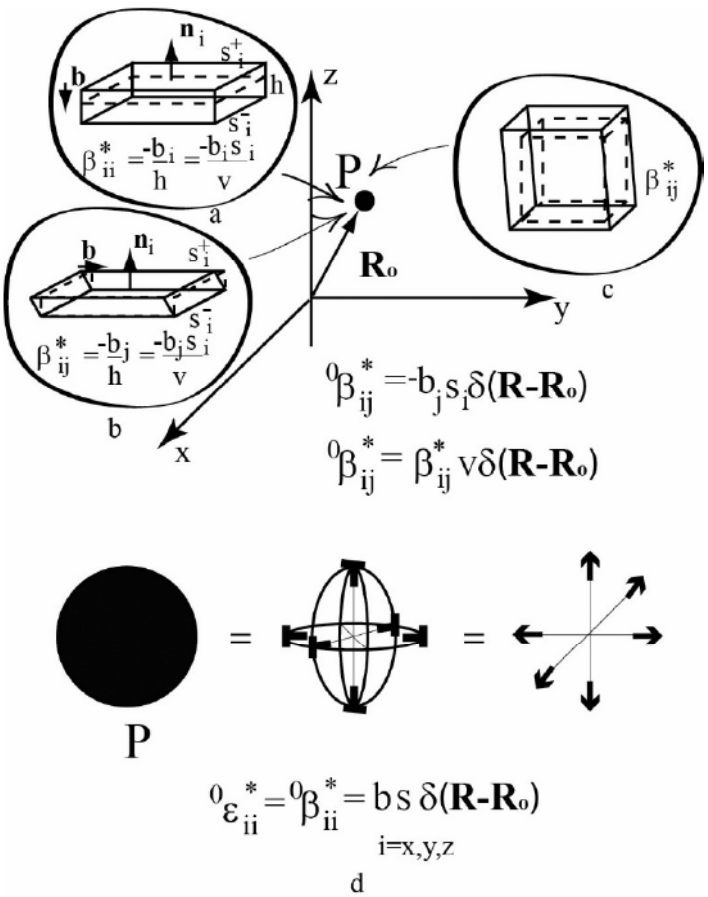

Fig. 1. Zero-dimensional defects in an elastic medium: (a) an infinitesimal prismatic dislocation loop; (b) an infinitesimal dislocation glide loop; (c) a general point defect. Self-distortions of defects ${}^0\beta^*_{ij}$ and *eigensrains* ${}^0\varepsilon^*_{ij}$ are shown. Reprinted with permission from A.L. Kolesnikova, R.M. Soroka,A.E. Romanov //Materials Physics andMechanics 17(1) (2013) 71, (c) 2013Advanced Study Center Co., Ltd.

example, in cylindrical or spherical ones ($i,j=r,\varphi,z$ or $i,j=R,\theta,\varphi$), respectively.

Equation (1) can be written in the general form:

$$ {}^0\beta^*_{ij} = \beta^*_{ij} v \delta(\mathbf{R}-\mathbf{R}_0), \quad i,j = x,y,z, \tag{2} $$

where β^*_{ij} is self-distortion of a small volume v without taking into account its location in an elastic medium (Fig. 1c).

Consider now the defects with a small cut surface s_z. The surfaces of the cut are subjected to arbitrary displacements written in the form of a combination of arbitrary shifts and rotations [10,22,23]:

$$ {}^0\beta^*_{ij} = \left\{-b_j - e_{jpq}\omega_p (x_q - x_{q0})\right\} s_z \delta(\mathbf{R}-\mathbf{R}_0), \tag{3} $$

where in curly brackets the shift of the upper part of the cut s_z^+ with respect to the fixed bottom part of the cut s_z^- is shown, b_j is the dislocation Burgers vector; e_{jpq} is the Levi-Civita tensor; ω_p is the disclination Frank pseudo-vector; x_{q0} is the axis of rotation. The sign of the distortion given by Eq. (3) is important. By definition, the Burgers vector is the disclosure vector for a Burgers circuit surrounding the defect line and crossing the selected cut surface s_z. The sign of the Burgers vector is related to the definition of the normal to the cut surface, the jump in the displacements at the cut, and, ultimately, the sign of self-distortion.

According to Eq. (3), we obtain infinitesimal dislocation-disclination loops with distortions written in the same way as for finite-dimensional dislocation-disclination loops [10], but stitched to the point (x_0,y_0,z_0).

Two kinds of infinitesimal dislocation loops, first investigated by Kroupa [5], are of particular interest. Using the Kroupa infinitesimal dislocation loops, as it will be shown below, it is possible to construct a point center of dilatation and some known defects of greater dimensions: dislocations, disclinations, and inclusions. If the vector is directed along the normal to the cut surface s_z, e.g. $\mathbf{b}=\pm b_z\mathbf{e}_z$, the infinitesimal loop is prismatic one (Fig. 1a). If the vector **b** lies in the plane of the cut, e.g. $\mathbf{b}=\pm b_x\mathbf{e}_x$, the infinitesimal loop is the glide dislocation loop (Fig. 1b).

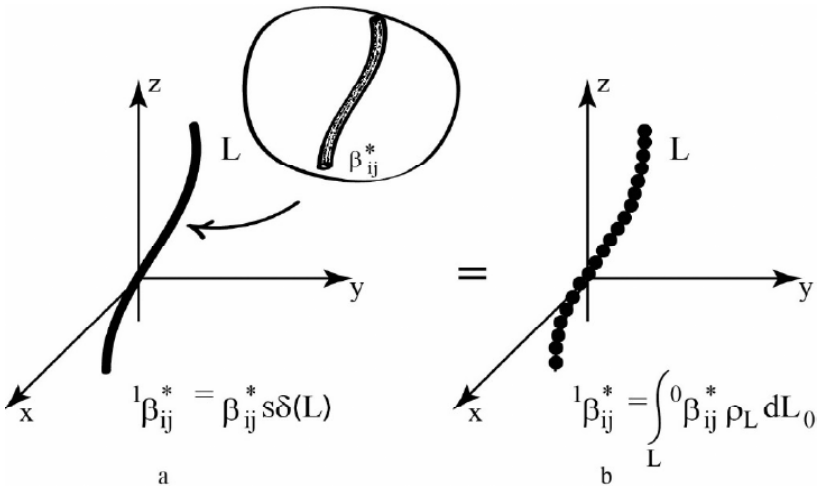

Fig. 2. One-dimensional defect (a) and its representation with the help of point defects (b), reprinted with permission from A.L. Kolesnikova, R.M. Soroka, A.E. Romanov // *Materials Physics and Mechanics* **17(1)** (2013) 71, (c) 2013 Advanced Study Center Co., Ltd.

For a dilatation center, the *eigenstrain* is given by

$$^0\varepsilon^*_{ii} = {}^0\beta^*_{ii} = -b_i s_i \delta(\mathbf{R}-\mathbf{R}_0), \quad i = x, y, z, \tag{4}$$

The dilatation center with *eigenstrain* $^0\varepsilon^*_{xx} = {}^0\varepsilon^*_{yy} = {}^0\varepsilon^*_{zz}$ is the simplest elastic model of an impurity atom or a vacancy, for which one can write [7] (Fig. 1d):

$$^0\varepsilon^*_{xx} = {}^0\varepsilon^*_{yy} = {}^0\varepsilon^*_{zz} = bs\delta(\mathbf{R}-\mathbf{R}_0) = \frac{1}{3}\Delta v\delta(\mathbf{R}-\mathbf{R}_0). \tag{5}$$

Here Δv is the change in volume at the point of defect localization. If l is the initial linear size of a small volume $v=l^3$, then changing the linear dimension by Δl leads to a change in the volume by $\Delta v = (l+\Delta l)^3 - l^3 \approx 3l^2\Delta l$. Assuming that $s=l^2$ and $b=\Delta l$, we obtain $bs=1/3(\Delta v)$ and the last equality in Eq. (5). Thus, the dilatation center can be represented by three mutually perpendicular infinitesimal prismatic dislocation loops (Fig. 2). Note, that three mutually perpendicular pairs of forces also model the dilatation center [18] (Fig. 1d).

An increase in the dimension of the region $\Omega_0 \to \Omega_1$ ($\Omega_1 \equiv L$), where defect is localized, leads to a one-dimensional defect.

One-dimensional defects (n=1). The distortion of a one-dimensional defect is logically to define as follows: cut a tube of small cross-section along the line **L** of the future defect, plastically deform the tube and insert it back into the cut, gluing the edges of the cut (Fig. 2a). As a result, the self-distortion of the one-dimensional defect is [21]:

$$^1\beta^*_{ij} = \beta^*_{ij} s\delta(L), \tag{6}$$

where β^*_{ij} is plastic distortion of **L**; s is multiplier having the dimension of an area; $\delta(L)$ is a two-dimensional delta-function.

One-dimensional defect can also be defined through zero-dimensional defects continuously distributed with prescribed linear density ρ_L along the line **L** (Fig. 2b):

$$^1\beta^*_{ij} = \int_L {}^0\beta^*_{ij}\rho_L \, dL_0 = \int_L \beta^*_{ij} v\delta(\mathbf{R}-\mathbf{R}_0)\rho_L(\mathbf{R}_0)\, dL_0, \quad i, j = x, y, z, \tag{7}$$

where L_0 is the coordinate of a probe point defect along the line **L**.

In the case when β^*_{ij} in Eq. (7) does not depend on the coordinate of the distributed point defects, i.e. their linear density is constant, we obtain a simple formula:

$$^1\beta^*_{ij} = \beta^*_{ij} v\rho_L \delta(L). \tag{8}$$

For a straight-line defect placed along the z-axis, $\delta(L)=\delta(x-x_0)\delta(y-y_0)$ and $[\delta(L)]=[\delta(x-x_0)][\delta(y-y_0)]=X^{-1}X^{-1}=X^{-2}$. Obviously, replacing $v\rho_L=s$ in Eq. (8) we arrive to Eq. (6). It follows from Eqs. (7) and (8) that by integrating the elastic fields of a zero-dimensional defect along the line with prescribed density, we can find the elastic fields of the particular one-dimensional defect. Representation of a one-dimensional defect via Eq. (7) has an explicit relationship with physical prototypes. For example, the linear distribution of distortions from Eq. (2) models a chain of vacancies or impurity atoms.

With a further increase in the dimension of the distortion-setting region $\Omega_1 \to \Omega_2$ ($\Omega_2 \equiv S$), we obtain two-dimensional defects, and, in particular, Somigliana and Volterra dislocations.

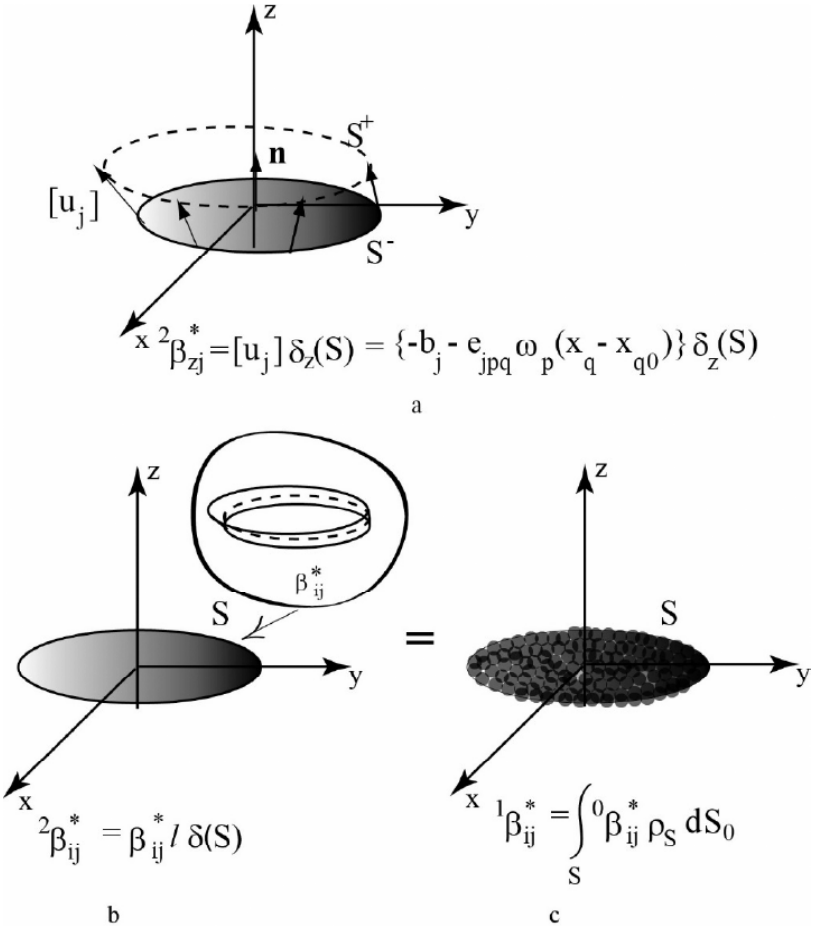

Fig. 3. Two-dimensional defect: (a) the Somigliana dislocation (in the special case, the Volterra dislocation), (b) the two-dimensional defect of the general form, (c) the two-dimensional defect composed of point defects, reprinted with permission from A.L. Kolesnikova, R.M. Soroka, A.E. Romanov // *Materials Physics and Mechanics* **17(1)** (2013) 71, (c) 2013 Advanced Study Center Co., Ltd.

Two-dimensional defects (n=2)**.** The region defining the eigenstrain (or self-distortion) of two-dimensional defects is the surface.

Somigliana dislocations and Volterra dislocations (i.e. translational dislocations and disclinations) are two-dimensional defects (Fig. 3à). For dislocation, the region of specifying its *eigenstrain* coincides with the surface of the cut, whose edges are subjected to relative displacements. Volterra dislocations do not have the discontinuity of the elastic strain/stress fields on the surface of the cut, but they have a singularity on the defect line bounding the surface of the cut. Therefore, they are traditionally called linear defects. The self-distortions for Somigliana and Volterra dislocations have the form (middle and right hand part in the formula, respectively) [22,23]:

$$^2\beta^*_{ij} = [u_j]\delta_i(S) = \left\{-b_j e_{jpq}\omega_p(x_q - x_{q0})\right\}\delta_i(S), \quad (9)$$

where $[u_j]$ is the jump of displacements specified on the surface of the cut S with the normal $\mathbf{n}_i$, $\delta_i(S)$ is the delta-function on the surface S: $\delta_i(S) = \int_S \delta(\mathbf{R} - \mathbf{R}_0)\,\mathrm{d}S'_i$. For a plane surface S with a normal $\mathbf{n}_z$, and a coordinate along the z-axis, we obtain $\delta(S)=\delta_z(S)\mathbf{e}_z=H(S)\delta(z-z_0)\mathbf{e}_z$, where $H(S) = \begin{cases} 1, & x,y \in S \\ 0, & x,y \notin S \end{cases}$ is the Heaviside step-function.

By analogy with Eqs. (2) and (6), for the two-dimensional defect of general form (Fig. 3b) the following expression can be written:

$$^2\beta^*_{ij} = \beta^*_{ij} l \delta(S), \quad (10)$$

where l is factor that has the dimension of length.

One can obtain a two-dimensional defect by distributing point defects on the surface S (Fig. 3c):

$$^2\beta^*_{ij} = \int_S {}^0\beta^*_{ij}\rho_s\,\mathrm{d}S_0 = \int_S \beta^*_{ij}(\mathbf{R}_0) v\delta(\mathbf{R} - \mathbf{R}_0)\rho_s(\mathbf{R}_0)\,\mathrm{d}S_0, \quad (11)$$

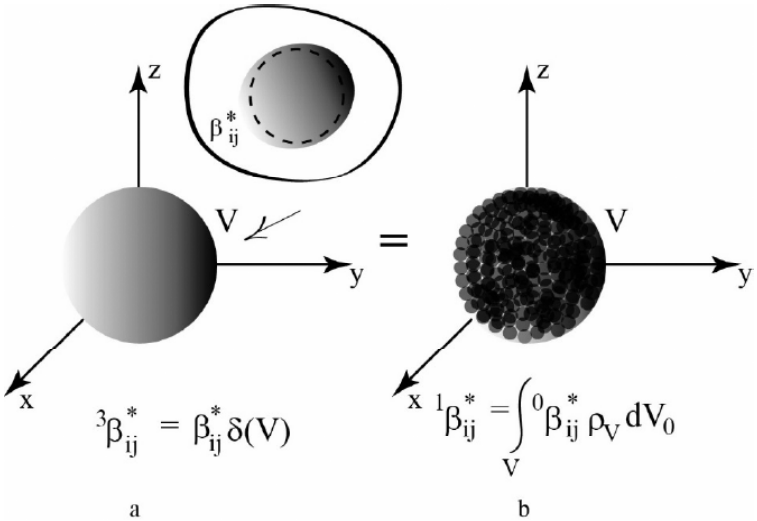

Fig. 4. The inclusion of the general form (a) and that composed of point defects (b), reprinted with permission from A.L. Kolesnikova, R.M. Soroka, A.E. Romanov // *Materials Physics and Mechanics* **17(1)** (2013) 71, (c) 2013 Advanced Study Center Co., Ltd.

where ρ_s is the surface density of distortions ${}^0\beta^*_{ij}$, S is the surface, over which the distortions are distributed. With constant $\beta^*_{ij}(\mathbf{R}_0)$ and $\rho_s(\mathbf{R}_0)$, and taking into account the relation $\rho_s v = l$, from Eq. (11) one gets Eq. (10).

With the help of distributed infinitesimal prismatic dislocation loops with self-distortions ${}^0\beta^*_{zz} = b_z s_z \delta(\mathbf{R}-\mathbf{R}_0)$, a finite prismatic dislocation loop located in the plane with the normal $\boldsymbol{n}_z$ and occupying the region S, is generated:

$$^2\beta^*_{ij} = \int_S {}^0\beta^*_{ij}\rho_s dS_0 = \int_S b_z s_z\, \delta(\mathbf{R}-\mathbf{R}_0)\rho_s dS_0 =$$

$$\int_S b_z s_z\, \delta(x-x_0)\delta(y-y_0)\delta(z-z_0)\rho_s dx_0 dy_0 =$$

$$b_z H(S)\delta(z-z_0) = b_z \delta_z(S).$$

Here it is assumed that $\rho_s = 1/s_z$.

The final step in the chain $\Omega_0 \to \Omega_1 \to \Omega_2 \to \Omega_3$ leads to volume defects.

Volume defects or inclusions (n=3). For inclusions, the *eigenstrain* ${}^3\varepsilon^*_{ij}$ or self-distortion ${}^3\beta^*_{ij}$ is written with the help of a volume delta function $\delta(\Omega_3) = \delta(V) = \begin{cases} 1, & \mathbf{R} \in V \\ 0, & \mathbf{R} \notin V \end{cases}$ [7] in the same way as it has been done in the previous cases (Fig. 4a):

$$^3\varepsilon^*_{ij} = \varepsilon^*_{ij}\delta(V),\ ^3\beta^*_{ij} = \beta^*_{ij}\delta(V),\ i,j = x,y,z. \qquad (12)$$

The components β^*_{ij} have the meaning of the relative elongation in the direction j of the elementary area with the normal $\mathbf{n}_j$ (at $i=j$) or the shift in the direction j of the elementary area with the normal $\mathbf{n}_j$ (at $i \neq j$). The eigenstrain ε^*_{ij} is a symmetrized distortion β^*_{ij}.

In a real crystal this means that, for example, as a result of a phase transition in the region Ω_3, the crystal lattice has changed its constants a_1, a_2, a_3 and, possibly, experienced some shear.

Note that the components of ε^*_{ij} and β^*_{ij} given by Eq. (12) need not necessarily be constant. A classical example of the inclusion of a not purely dilatational type is a particle with the intrinsic deformation of Marks-Ioffe [24], embedded in the matrix.

An inclusion can be composed of defects of lower dimension. For example, continuously distributed point defects form the inclusion characterized by Eq. (12), see Fig. 4b:

$$^3\beta^*_{ij} = \int_V {}^0\beta^*_{ij}\rho_V dV_0 =$$

$$\int_V \beta^*_{ij}(\mathbf{R}_0)v\delta(\mathbf{R}-\mathbf{R}_0)\rho_V dV_0 = \beta^*_{ij}(\mathbf{R}_0)\delta(V), \qquad (13)$$

where $\rho_V = 1/v$.

It is not difficult to see that in a 3D continuum, the defects of a dimension lower than 3 have self-distortions with some arbitrary dimensional factors. For the point defect, this is v in Eq. (2), for the linear defect – s in Eq. (6), and for the 2D-defect – l in Eq. (10). For definiteness, we can consider such a factor as the defect size before plastic deformation. So, v is the volume of the point, s is the cross-sectional area of the line, and l is the thickness of the 2D-defect.

3. ELASTIC FIELDS OF DEFECTS IN 3D MEDIUM

By using the self-distortion ${}^{n}\beta^{*}_{ij}$ (or the *eigenstrain* ${}^{n}\varepsilon^{*}_{ij}$) of the defect, the Green function G_{mk} and elastic moduli C_{jlmn} of the elastic medium, the total displacements of the defect, as well as its elastic strains and stresses can be found (see [7,10]).
For example, the total displacements of defect are given by the following equation [7]:

$$u_i^t(\mathbf{R}) = -\int_V C_{jlmn}\,{}^{n}\varepsilon^{*}_{mn}(\mathbf{R}')G_{ij,l}(|\mathbf{R}-\mathbf{R}'|)dV', \tag{14}$$

where the derivative $G_{ij,l}(\mathbf{R}\text{-}\mathbf{R}')$ is taken over the unprimed variable x_1, V is the volume of a solid, and the summation is made over repeated indices. Note that $\partial G_{ij}/\partial x_l = -\partial G_{ij}/\partial x_l'$ and, therefore, Eq. (14) can also be written with the plus sign before the integral, bearing in mind the differentiation over the primed coordinate x_l'. Taking into account the relations ${}^{n}\varepsilon^{*}_{mn}={}^{n}\varepsilon^{*}_{nm}=1/2\,({}^{n}\beta^{*}_{mn}+{}^{n}\beta^{*}_{nm})={}^{n}\beta^{*}_{(nm)}$ and $C_{jlmn}=C_{jlnm}$, the substitution ${}^{n}\varepsilon^{*}_{mn}(\mathbf{R}')\to{}^{n}\beta^{*}_{mn}(\mathbf{R}')$ in Eq. (14) can be done. Here, the upper left index n indicates the dimension of the defect.

For an isotropic 3D elastic medium, the Green function and term $C_{jlmn}G_{ij,k}(|\mathbf{R}\text{-}\mathbf{R}'|)$ are expressed in the forms [10]:

$$G_{ij}(|\mathbf{R}-\mathbf{R}'|) = \frac{1}{16\pi G(1-\nu)|\mathbf{R}-\mathbf{R}'|}\left\{(3-4\nu)\delta_{ij}+\frac{(x_i-x_i')(x_j-x_j')}{|\mathbf{R}-\mathbf{R}'|^2}\right\}, \tag{15a}$$

$$C_{jlmn}G_{ij,l}(|\mathbf{R}-\mathbf{R}'|) == -\frac{1}{8\pi(1-\nu)}\times$$
$$\left\{(1-2\nu)\frac{\delta_{mi}(x_n-x_n')+\delta_{ni}(x_m-x_m')-\delta_{mn}(x_i-x_i')}{|\mathbf{R}-\mathbf{R}'|^3}+3\frac{(x_n-x_n')(x_m-x_m')(x_i-x_i')}{|\mathbf{R}-\mathbf{R}'|^5}\right\}. \tag{15b}$$

Here $|\mathbf{R}-\mathbf{R}'| = \sqrt{(x-x')^2+(y-y')^2+(z-z')^2}$; x_n, x_m, x_i are x, y, and z; δ_{km} is the Kronecker delta, G is the shear modulus, and ν is the Poisson ratio.

Equations (14) and (15) are convenient for calculating the displacements of point defects. For defects of higher dimension, the formulas for displacements can be simplified by applying to them the direct and inverse Fourier transformations [22]. As a result, the universal working formula relating the self-distortion of the defect with its displacement field, takes the form [22]:

$$u_i^t(\mathbf{R}) = -i\int\int_{-\infty}^{\infty}\xi_l C_{jlmn}\hat{G}_{ij}\,{}^{n}\hat{\beta}^{*}_{mn}\exp(i\,\boldsymbol{\xi}\cdot\mathbf{R})d\xi_x d\xi_y d\xi_z, \tag{16}$$

where $\hat{G}_{ij}$ and ${}^{n}\hat{\beta}^{*}_{ij}$ are Fourier transforms of the Green function of the elastic medium and the self-distortion (*eigenstrain*) of the defect, respectively; $\xi\mathbf{R}=\xi_x x+\xi_y y+\xi_z z$.

For an isotropic medium, the terms of Eq. (16) are known [22]:

$$C_{jlmn} = \frac{2G\nu}{1-2\nu}\delta_{jl}\delta_{mn}+G\left(\delta_{lm}\delta_{jn}+\delta_{ln}\delta_{jm}\right), \tag{17a}$$

$$\hat{G}_{ij} = \frac{1}{(2\pi)^{3/2}}\frac{2(1-\nu)\xi^2\delta_{ij}-\xi_i\xi_j}{2(1-\nu)G\xi^4}, \tag{17b}$$

where $\xi^2=\xi_x^2+\xi_y^2+\xi_z^2$.

Thus, the way to find the elastic fields of an arbitrary defect is simple: one should take its *eigenstrain* and apply a well known formula, e. g., Eq. (14) or Eq. (16), to it.

Sometimes, however, it is easier to act in a different manner, by integrating the field of one defect of lower dimension to get the field of a defect of higher dimension. For example, based on of the field of the point dilatation center given by Eq. (14), we find the fields of other dilatation sources in the form of segment, straight line, circular line, circular disk, and axisymmetric inclusions [21,25]. In doing so, first, we find the

fields of an infinitesimal prismatic dislocation loop (IPDL) and compare them with the fields represented by Kroupa [5].

3.1. Infinitesimal prismatic dislocation loop (IPDL)

Consider an IPDL placed at the beginning of the Cartesian coordinate system and characterized by the following *eigenstrain*:

$$ {}^{0}\varepsilon_{zz}^{*IDPL} = {}^{0}\beta_{zz}^{*IDPL} = bs\delta(\mathbf{R}). \tag{18}$$

The field of total displacements of this loop $u_i^{IPDL}(\mathbf{R})$, calculated by using Eqs. (14), (15), and (18), reads:

$$u_x^{IPDL} = \frac{bs\ x}{8\pi(1-\nu)\,|\mathbf{R}|^3}\left\{-(1-2\nu)+3\frac{z^2}{|\mathbf{R}|^2}\right\}, \tag{19a}$$

$$u_y^{IPDL} = \frac{bs\ y}{8\pi(1-\nu)\,|\mathbf{R}|^3}\left\{-(1-2\nu)+3\frac{z^2}{|\mathbf{R}|^2}\right\}, \tag{19b}$$

$$u_z^{IPDL} = \frac{bs\ z}{8\pi(1-\nu)\,|\mathbf{R}|^3}\left\{(1-2\nu)+3\frac{z^2}{|\mathbf{R}|^2}\right\}, \tag{19c}$$

where $|\mathbf{R}| = \sqrt{x^2+y^2+z^2}$.

The displacements allow us to calculate the elastic strain field $\varepsilon_{ij} = 1/2(\partial u_j/\partial x_i + \partial u_i/\partial x_j) - {}^{n}\varepsilon_{ij}^{*}$, and then, through the Hooke law, $\sigma_{ij} = 2G(\varepsilon_{ij} + (\nu/(1-2\nu))\Delta\delta_{ij})$, $\Delta=\varepsilon_{xx}+\varepsilon_{yy}+\varepsilon_{zz}$, $i,j= x,y,z$, the stress field:

$$\sigma_{xx}^{IPDL} = \frac{3Gbs}{4\pi(1-\nu)\,|\mathbf{R}|^3}\times \left\{\frac{4\nu-1}{3}+(1-2\nu)\frac{x^2+z^2}{|\mathbf{R}|^2}-5\frac{x^2z^2}{|\mathbf{R}|^4}\right\}, \tag{20a}$$

$$\sigma_{yy}^{IPDL} = \frac{3Gbs}{4\pi(1-\nu)\,|\mathbf{R}|^3}\times \left\{\frac{4\nu-1}{3}+(1-2\nu)\frac{y^2+z^2}{|\mathbf{R}|^2}-5\frac{y^2z^2}{|\mathbf{R}|^4}\right\}, \tag{20b}$$

$$\sigma_{zz}^{IPDL} = \frac{3Gbs}{4\pi(1-\nu)\,|\mathbf{R}|^3}\times \left\{\frac{1}{3}+2\frac{z^2}{|\mathbf{R}|^2}-5\frac{z^4}{|\mathbf{R}|^4}\right\}, \tag{20c}$$

$$\sigma_{xy}^{IPDL} = \frac{3Gbs\ xy}{4\pi(1-\nu)\,|\mathbf{R}|^5}\left\{1-2\nu-5\frac{z^2}{|\mathbf{R}|^2}\right\}, \tag{20d}$$

$$\sigma_{xz}^{IPDL} = \frac{3Gbs\ xz}{4\pi(1-\nu)\,|\mathbf{R}|^5}\left\{1-5\frac{z^2}{|\mathbf{R}|^2}\right\}, \tag{20e}$$

$$\sigma_{yz}^{IPDL} = \frac{3Gbs\ yz}{4\pi(1-\nu)\,|\mathbf{R}|^5}\left\{1-5\frac{z^2}{|\mathbf{R}|^2}\right\}. \tag{20f}$$

The calculated fields (19) and (20) are in accordance with the fields given in [5]. We note that in order to find the elastic strains, we differentiated the total displacements (19), ignoring the singularity point (0,0,0).

3.2. Center of dilatation (ΔP)

Combining the fields of three mutually perpendicular IPDLs, given by Eqs. (19) and (20), we find the fields of the point dilatation source (Fig. 2) as:

$$u_x^{\Delta P} = \frac{(1+\nu)bs}{4\pi(1-\nu)}\cdot\frac{x}{|\mathbf{R}|^3}, \tag{21a}$$

$$u_y^{\Delta P} = \frac{(1+\nu)bs}{4\pi(1-\nu)}\cdot\frac{y}{|\mathbf{R}|^3}, \tag{21b}$$

$$u_z^{\Delta P} = \frac{(1+\nu)bs}{4\pi(1-\nu)}\cdot\frac{z}{|\mathbf{R}|^3}; \tag{21c}$$

$$\sigma_{xx}^{\Delta P} = \frac{G(1+\nu)bs}{2\pi(1-\nu)}\cdot\frac{(-2x^2+y^2+z^2)}{|\mathbf{R}|^5}, \tag{22a}$$

$$\sigma_{yy}^{\Delta P} = \frac{G(1+\nu)bs}{2\pi(1-\nu)}\cdot\frac{(x^2-2y^2+z^2)}{|\mathbf{R}|^5}, \tag{22b}$$

$$\sigma_{xx}^{\Delta P} = \frac{G(1+\nu)bs}{2\pi(1-\nu)}\cdot\frac{(x^2+y^2-2z^2)}{|\mathbf{R}|^5}, \tag{22c}$$

$$\sigma_{xy}^{\Delta P} = -\frac{3G(1+\nu)bs}{2\pi(1-\nu)}\cdot\frac{xy}{|\mathbf{R}|^5}, \tag{22d}$$

$$\sigma_{xy}^{\Delta P} = -\frac{3G(1+\nu)bs}{2\pi(1-\nu)}\cdot\frac{xz}{|\mathbf{R}|^5}, \tag{22e}$$

$$\sigma_{xy}^{\Delta P} = -\frac{3G(1+\nu)bs}{2\pi(1-\nu)}\cdot\frac{yz}{|\mathbf{R}|^5}, \tag{22f}$$

$$\sigma_{xx}^{\Delta P} + \sigma_{yy}^{\Delta P} + \sigma_{zz}^{\Delta P} = 0. \tag{22g}$$

3.3. The dilatation segment (ΔL), the dilatation ray (ΔLi), and the dilatational straight line ($\Delta Line$)

Integrating the fields of the dilatation center along the straight line within the given limits, we obtain the fields of the dilatational segment. For example, the stress field of the segment oriented along the z-axis is:

$$\sigma_{ij}^{\Delta L} = \int_{z_1}^{z_2} \sigma_{ij}^{\Delta P}(x, y, z - z_0)\rho \, \mathrm{d}z_0, \tag{23}$$

where ρ is the linear density of the distribution of point defects. The stress components (23) have an analytic representation via elementary functions.

From the stress field (23) of a segment, with limiting transition $z_2 \to \infty$ we find the stress field of the dilatation ray emerging from the coordinate origin (0,0,0). For z_1=0 it reads:

$$\sigma_{xx}^{\Delta Li} = -\frac{G(1+\nu)\rho bs}{2\pi(1-\nu)}\left(\frac{x^2 - y^2}{(x^2+y^2)^2} + \frac{z(2x^4 + x^2(y^2+z^2) - y^2(y^2+z^2))}{|\mathbf{R}|^3\,(x^2+y^2)^2}\right), \tag{24a}$$

$$\sigma_{yy}^{\Delta Li} = -\frac{G(1+\nu)\rho bs}{2\pi(1-\nu)}\left(\frac{y^2 - x^2}{(x^2+y^2)^2} + \frac{z(2y^4 + y^2(x^2+z^2) - x^2(x^2+z^2))}{|\mathbf{R}|^3\,(x^2+y^2)^2}\right), \tag{24b}$$

$$\sigma_{zz}^{\Delta Li} = \frac{G(1+\nu)\rho bs}{2\pi(1-\nu)}\frac{z}{|\mathbf{R}|^3}, \tag{24c}$$

$$\sigma_{xy}^{\Delta Li} = -\frac{G(1+\nu)\rho bs}{2\pi(1-\nu)}\left(\frac{2xy}{(x^2+y^2)^2} + \frac{xyz(3x^2+3y^2+2z^2)}{(x^2+y^2)^2\,|\mathbf{R}|^3}\right), \tag{24d}$$

$$\sigma_{xz}^{\Delta Li} = \frac{G(1+\nu)\rho bs}{2\pi(1-\nu)}\frac{x}{|\mathbf{R}|^3}, \tag{24e}$$

$$\sigma_{yz}^{\Delta Li} = \frac{G(1+\nu)\rho bs}{2\pi(1-\nu)}\frac{y}{|\mathbf{R}|^3}. \tag{24f}$$

In addition, from the fields (24) of the segment, in the limiting transitions $z_1 \to -\infty$ and $z_2 \to \infty$, one can find the stress field of an infinite dilatational straight line directed along the z-axis:

$$\sigma_{xx}^{\Delta Line} = -\frac{G(1+\nu)\rho bs}{\pi(1-\nu)}\frac{(x^2 - y^2)}{(x^2+y^2)^2}, \tag{25a}$$

$$\sigma_{yy}^{\Delta Line} = -\frac{G(1+\nu)\rho bs}{\pi(1-\nu)}\frac{(y^2 - x^2)}{(x^2+y^2)^2}, \tag{25b}$$

$$\sigma_{xy}^{\Delta Line} = -\frac{G(1+\nu)\rho bs}{\pi(1-\nu)}\frac{2xy}{(x^2+y^2)^2}, \tag{25c}$$

$$\sigma_{zz}^{\Delta Line} = \sigma_{xz}^{\Delta Line} = \sigma_{yz}^{\Delta Line} = 0. \tag{25d,e,f}$$

In the cylindrical coordinate system (r,φ,z), the stress tensor (25) can be written as

$$\sigma_{rr}^{\Delta Line} = -\sigma_{\varphi\varphi}^{\Delta Line} = -\frac{G(1+\nu)\rho bs}{\pi(1-\nu)} \cdot \frac{1}{r^2}, \tag{26a,b}$$

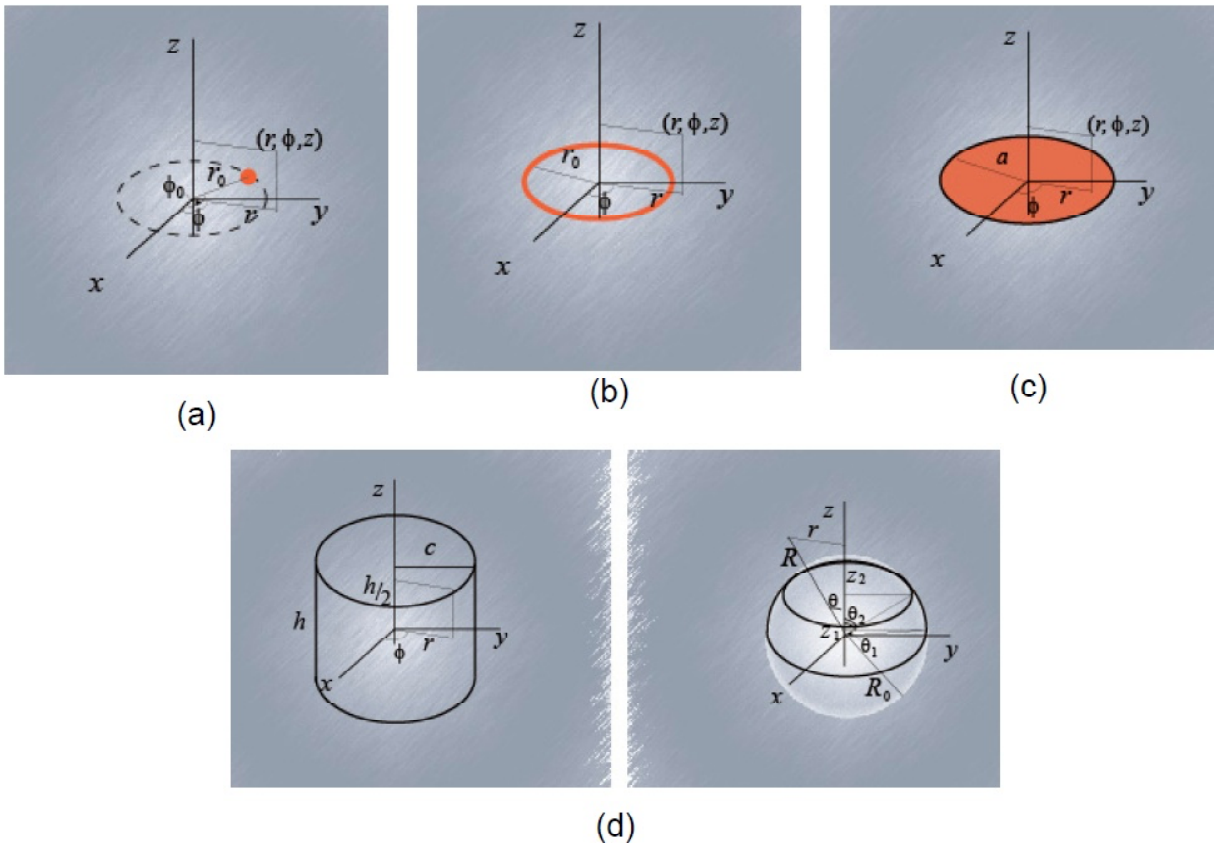

Fig. 5. From a point defect to an axisymmetric inclusion. (a) The point defect (red); (b) the circular line; (c) the circular disk, and (d) the axisymmetric inclusion.

$$\sigma_{zz}^{\Delta Line} = \sigma_{r\varphi}^{\Delta Line} = \sigma_{rz}^{\Delta Line} = \sigma_{z\varphi}^{\Delta Line} = 0. \qquad (26c\text{-}f)$$

In Eqs. (26 a,b), we can introduce a cutoff radius ξ around the singular point r=0 and rewrite the coefficient at $1/r^2$ as

$$-\frac{G(1+\nu)\rho bs}{\pi(1-\nu)} = -\frac{G(1+\nu)\rho_{\Delta V}}{3\pi(1-\nu)} =$$
$$-\frac{G(1+\nu)\rho_{\Delta V}\xi^2}{3(1-\nu)\pi\xi^2} = -\frac{G(1+\nu)_{\Delta V}\xi^2}{3(1-\nu)_V},$$

thus finding the stress field caused by a cylindrical inclusion with a small core. This inclusion simulates an actual inclusion of cylindrical shape in the case when the inclusion radius is small as comparing with other size parameters of the problem. Such a model is adopted, for example, when considering the elastic behavior of the Abrikosov flux line in Type II superconductors [26]. The Abrikosov flux line is a cylindrical region of the normal phase, surrounded by a superconducting phase. A similar model was used to model the phason imperfections in quasiperiodic grain boundaries in crystalline solids [27].

3.4. Circular dilatation line ($C\Delta L$)

Egenstrain tensor of the dilatation center [see Eq. (4)] in the cylindrical coordinate system (r,φ,z) has the form:

$$^0\varepsilon_{rr}^* = {}^0\varepsilon_{\varphi\varphi}^* = {}^0\varepsilon_{zz}^* = bs\,\delta(x-x_0)\delta(y-y_0)\delta(z) =$$
$$bs\frac{1}{r_0}\delta(r-r_0)\delta(\varphi-\varphi_0)\delta(z), \qquad (27)$$

where (x_0,y_0,0) and (r_0,φ_0,0) are the dilatation center coordinates in the Cartesian and cylindrical coordinate systems, respectively (Fig. 5a).

Let us distribute the point centers of the dilatation along a circle of radius r_0 with a constant linear density ρ (Fig. 5b). As a result, we obtain a circular dilatation line ($C\Delta L$**)**. In the cylindrical coordinate system (r,φ,z), the *eigenstrain* tensor of $C\Delta L$ is written as:

$$^1\varepsilon_{rr}^* = {}^1\varepsilon_{\varphi\varphi}^* = {}^1\varepsilon_{zz}^* = \int_0^{2\pi} bs\frac{1}{\cancel{r_0}}\delta(r-r_0)\times$$
$$\delta(\varphi-\varphi_0)\delta(z)\rho\cancel{r_0}\,d\varphi_0 = bs\rho\delta(r-r_0)\delta(z). \qquad (28)$$

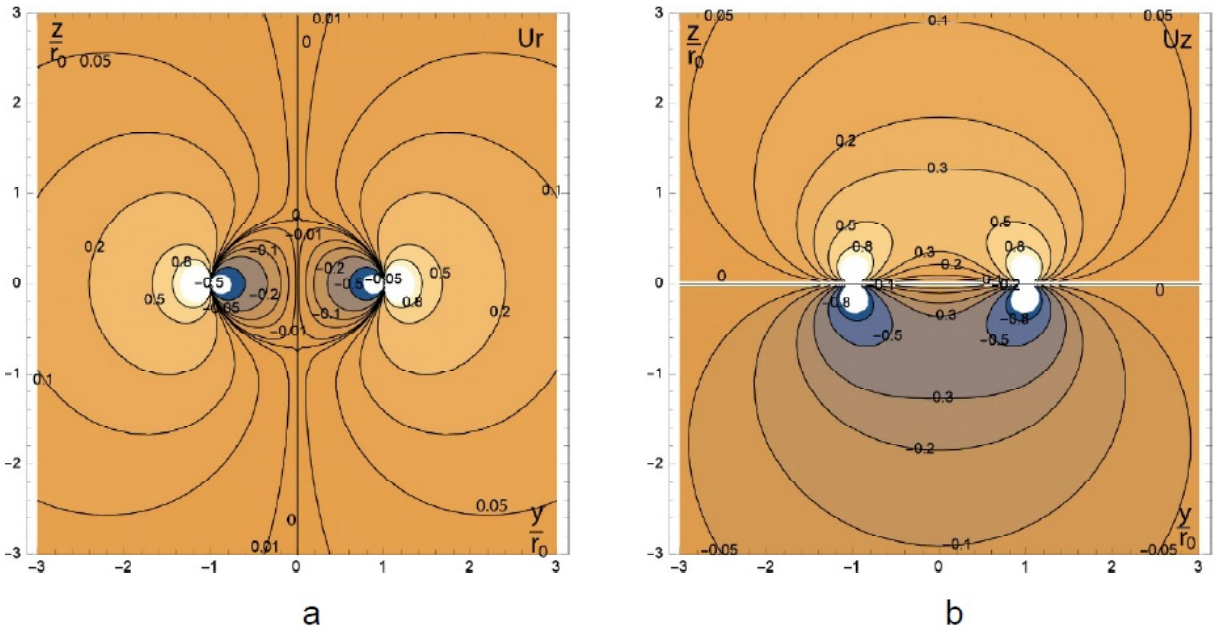

Fig. 6. Maps of displacements of a circular dilatation line. The maps are built in the plane x=0. The displacement values are given in units of $((1+\nu)\rho bs)/(2\pi(1-\nu)r_0)$ and the coordinates are normalized to the circle radius r_0. Here ρ is the density of the dilatation centers that form the circular line; b and s are the values of the small Burgers vector and the area of infinitesimal prismatic loops forming the dilatation center, respectively; ν is the Poisson ratio.

The displacements of the circular dilatation line can be calculated by integrating the displacements (21) of the dilatation center with the coordinates $(r_0,\varphi_0,0)$ along the circle, the element of which is $dl=r_0 d\varphi_0$, from 0 to 2π with the weight ρ:

$$u_i^{C\Delta L} = \int_0^{2\pi} u_i^{\Delta P} \rho r_0 \, \mathrm{d}\varphi_0, \quad i = r, \varphi, z. \tag{29}$$

The integration gives

$$u_r^{C\Delta L} = \frac{(1+\nu)\rho bs}{2\pi(1-\nu)} \cdot \frac{r_0 k}{8r^{5/2}(-r_0)^{3/2}(1-k^2)} \times \left[k^2(r^2 - r_0^2 - z^2)\mathbf{E}(k) + 4(-rr_0)(1-k^2)\mathbf{K}(k)\right], \tag{30a}$$

$$u_\varphi^{C\Delta L} = 0, \tag{30b}$$

$$u_z^{C\Delta L} = \frac{(1+\nu)\rho bs}{2\pi(1-\nu)} \cdot \frac{r_0 z k^3}{4(1-k^2)(-rr_0)^{3/2}} \mathbf{E}(k), \tag{30c}$$

where

$$\mathbf{K}(k) = \int_0^{2\pi} \frac{\mathrm{d}t}{\sqrt{1-k^2\sin^2 t}} \quad \text{and}$$

$$\mathbf{E}(k) = \int_0^{2\pi} \sqrt{1-k^2\sin^2 t}\, \mathrm{d}t$$

are the complete elliptic integrals of the first and second kind [28], respectively, and

$$k = \frac{2\sqrt{-r\, r_0}}{\sqrt{z^2 + (r - r_0)^2}}.$$

Displacements (30) can be rewritten in terms of the Lipschitz-Hankel integrals

$$J(m,n;p) = \int_0^\infty J_m(\kappa) J_n\left(\tfrac{r}{r_0}\kappa\right) e^{-|z|\kappa/r_0} \kappa^p \, \mathrm{d}\kappa$$

[29], where $J_n(\lambda)$ are the Bessel functions of the first kind [28], as follows:

$$u_r^{C\Delta L} = \frac{(1+\nu)\rho bs}{2(1-\nu)} \cdot \frac{1}{r_0} J(0,1;1), \tag{31a}$$

$$u_\varphi^{C\Delta L} = 0, \tag{31b}$$

$$u_z^{C\Delta L} = \frac{(1+\nu)\rho bs}{2(1-\nu)} \cdot \frac{\mathrm{sgn}(z)}{r_0} J(0,0;1), \tag{31c}$$

where sgn(z)={1, z>0; 0, z=0; -1, z<0}.

In Fig. 6, the field of total displacements for a circular dilatation line is shown.

The displacements (31) give a possibility to find the elastic strains ε_{ij} and stresses σ_{ij} in the cylindri-

cal coordinate system by using the following equations taking into account *eigenstrain* ${}^{n}\varepsilon^{*}_{ij}$ [18]:

$$\varepsilon_{rr} = \frac{\partial u_r}{\partial r} - {}^{n}\varepsilon^{*}_{rr}, \tag{32a}$$

$$\varepsilon_{\varphi\varphi} = \frac{\partial u_\varphi}{r\,\partial\varphi} + \frac{u_r}{r} - {}^{n}\varepsilon^{*}_{\varphi\varphi}, \tag{32b}$$

$$\varepsilon_{zz} = \frac{\partial u_z}{\partial z} - {}^{n}\varepsilon^{*}_{zz}, \tag{32c}$$

$$\varepsilon_{rz} = \frac{1}{2}\left(\frac{\partial u_z}{\partial r} + \frac{\partial u_r}{\partial z}\right), \tag{32d}$$

$$\varepsilon_{r\varphi} = \frac{1}{2}\left(\frac{\partial u_\varphi}{\partial r} + \frac{\partial u_r}{\partial\varphi}\cdot\frac{1}{r} - \frac{u_\varphi}{r}\right), \tag{32e}$$

$$\varepsilon_{\varphi z} = \frac{1}{2}\left(\frac{\partial u_z}{\partial\varphi}\cdot\frac{1}{r} + \frac{\partial u_\varphi}{\partial z}\right), \tag{32f}$$

and the Hooke law $\sigma_{ij} = 2G(\varepsilon_{ij}+(\nu/(1-2\nu))\Delta\delta_{ij})$, $i,j = r,\lambda,z$ [30], where $\Delta=\varepsilon_{rr}+\varepsilon_{jj}+\varepsilon_{zz}$.
Here, for $C\Delta L$ ${}^{n}\varepsilon^{*}_{ij} = {}^{1}\varepsilon^{*}_{ij}$, see Eq. (28).

The resulting stresses of $C\Delta L$ satisfy the equilibrium equations.

3.5. Circular dilatation disk (*C*Δ*D*)

The elastic fields of a circular dilatational disk (*C*Δ*D*) can be calculated by integrating the elastic fields of a $C\Delta L$ along the radius r_0 from 0 to *a* with a constant density ρ (Fig. 5c).

The displacements can be written as:

$$u_i^{C\Delta D} = \int_0^a u_i^{C\Delta L}\rho\,\mathrm{d}r_0, \quad i = r,\varphi,z \tag{33}$$

that gives

$$u_r^{C\Delta D} = \frac{(1+\nu)b}{2(1-\nu)}J(1,1;0), \tag{34a}$$

$$u_\varphi^{C\Delta D} = 0, \tag{34b}$$

$$u_z^{C\Delta D} = \frac{(1+\nu)b}{2(1-\nu)}\mathrm{sgn}(z)J(1,0;0). \tag{34c}$$

In Fig. 7, the maps of total displacements for a circular dilatation disk are shown.

The elastic strains ε_{ij} and stresses σ_{ij} of a *CDD* can be calculated by Eqs. (32) and the Hooke law taking into account ${}^{n}\varepsilon^{*}_{ij} = {}^{2}\varepsilon^{*}_{ij}$,:

$${}^{2}\varepsilon^{*}_{rr} = {}^{2}\varepsilon^{*}_{\varphi\varphi} = {}^{2}\varepsilon^{*}_{zz} = b\,H(1-\frac{r}{a})\delta(z), \tag{35}$$

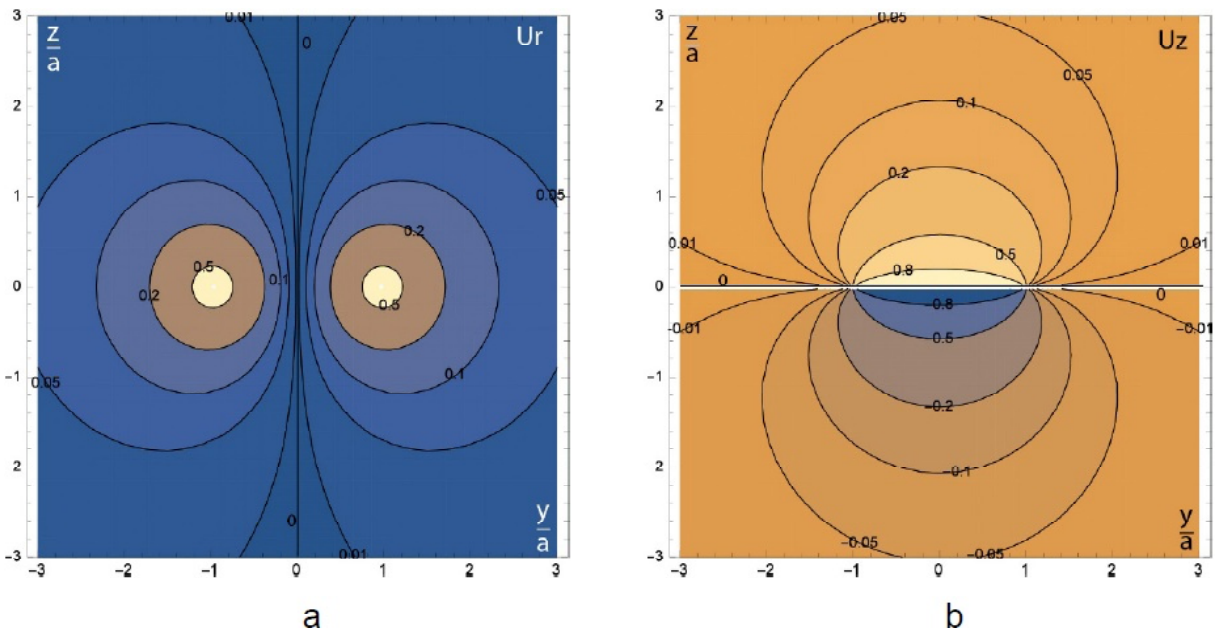

Fig. 7. Maps of displacements of a circular dilatation disk located in the *xy*-plane. The maps are built in the plane *x*=0. Displacements are given in units of $((1+\nu)b)/(2\pi(1-\nu))$ and the coordinates are normalized to the disk radius *a*. Here *b* is the value of the small Burgers vector of infinitesimal prismatic loops forming the dilatation centers which in turn form the dilatation disk; ν is the Poisson ratio.

where $H(1-r/a)$ is Heaviside step function.

3.6. Axisymmetric dilatational inclusions

With continuously distribution of the dilatational disks along the z-axis, we can construct axisymmetric inclusions (Fig. 5d) and calculate their elastic fields [25]. For example, *eigenstrain* and the displacement field of a cylindrical dilatational inclusion of finite height can be written as:

$$^{3}\varepsilon_{ii}^{*} = \varepsilon^{*}\begin{cases} 1, \text{ inside inclusion} \\ 0, \text{ outside inclusion} \end{cases}; \tag{36}$$

inside inclusion ($r<c$, $-h/2<z<h/2$):

$$u_r^{in} = \frac{(1+\nu)\varepsilon^{*}c}{2(1-\nu)}\left[\frac{r}{c} - J^{(1)}(1,1;-1) - J^{(2)}(1,1;-1)\right], \tag{37a}$$

$$u_\varphi^{in} = 0, \tag{37b}$$

$$u_z^{in} = \frac{(1+\nu)\varepsilon^{*}c}{2(1-\nu)}\operatorname{sgn}(z)\left[J^{(1)}(1,0;-1) - J^{(2)}(1,0;-1)\right]; \tag{37c}$$

outside inclusion ($z>h/2$, or $z<-h/2$, or $-h/2\le z\le h/2$ and $r>c$):

$$u_r^{out} = \frac{(1+\nu)\varepsilon^{*}c}{2(1-\nu)}\begin{cases} \left[J^{(3)}(1,1;-1) - J^{(2)}(1,1;-1)\right], & z < -\frac{h}{2} \text{ or } z > \frac{h}{2} \\ \left[\frac{c}{r} - J^{(1)}(1,1;-1) - J^{(2)}(1,1;-1)\right], & -\frac{h}{2} \le z \le \frac{h}{2} \text{ and } r > c \end{cases}, \tag{38a}$$

$$u_\varphi^{out} = 0, \tag{38b}$$

$$u_z^{out} = \frac{(1+\nu)\varepsilon^{*}c}{2(1-\nu)}\operatorname{sgn}(z)\begin{cases} \left[J^{(3)}(1,0;-1) - J^{(2)}(1,0;-1)\right], & z < -\frac{h}{2} \text{ or } z > \frac{h}{2} \\ \left[J^{(1)}(1,0;-1) - J^{(2)}(1,0;-1)\right], & -\frac{h}{2} \le z \le \frac{h}{2} \text{ and } r > c \end{cases}. \tag{38c}$$

Here the Lipschitz-Hankel integrals have the following forms:

$$J^{(1)}(m,n;p) = \int_0^\infty J_m(\kappa)J_n\left(\kappa\frac{r}{c}\right)e^{-\kappa\xi_1}\kappa^p d\kappa, \quad \xi_1 = \frac{\frac{h}{2} - |z|}{c}, \tag{39a}$$

$$J^{(2)}(m,n;p) = \int_0^\infty J_m(\kappa)J_n\left(\kappa\frac{r}{c}\right)e^{-\kappa\xi_2}\kappa^p d\kappa, \quad \xi_2 = \frac{\frac{h}{2} + |z|}{c}, \tag{39b}$$

$$J^{(3)}(m,n;p) = \int_0^\infty J_m(\kappa)J_n\left(\kappa\frac{r}{c}\right)e^{-\kappa\xi_3}\kappa^p d\kappa, \quad \xi_3 = \frac{|z| - \frac{h}{2}}{c}, \tag{39c}$$

Note that $\xi_1>0$ for $-h/2\le z\le h/2$, $\xi_2>0$ for any z, and $\xi_3>0$ for $z>h/2$ or $z<-h/2$; c and h are the radius and the height of the cylinder, respectively.

Fig. 8 shows the field of total displacements of the cylindrical dilatational inclusion in the central longitudinal section $x = 0$. The field of elastic strains is determined from the field of total displacements given by Eqs. (37)-(38) and relations (32), when

$$^{n}\varepsilon_{ii}^{*} = {}^{3}\varepsilon_{ii}^{*} = \varepsilon^{*}\begin{cases} 1, \text{ inside inclusion} \\ 0, \text{ outside inclusion} \end{cases}.$$

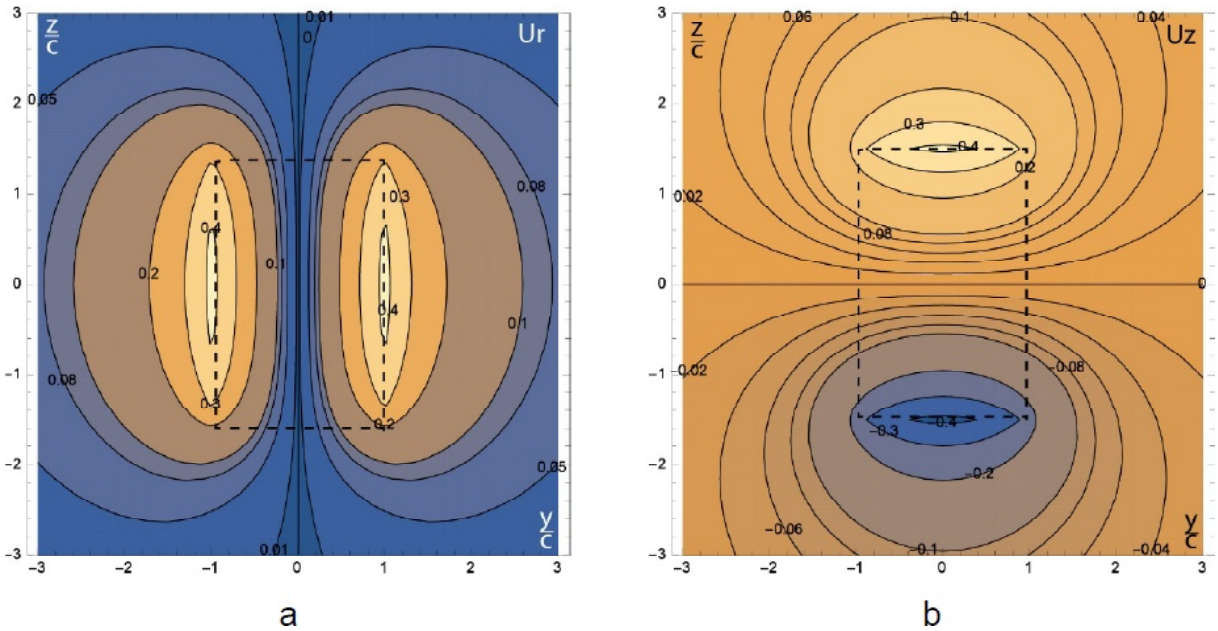

Fig. 8. Maps of the displacements of a cylindrical dilatational inclusion: (a) radial displacement u_r, (b) axial displacement u_z. The inclusion axis coincides with the *z*-axis. The displacement maps are built in the central longitudinal section $x = 0$ of the inclusion. Displacement values are given in units of $((1+\nu)\varepsilon^* c)/(1-\nu)$, where ε^* is the *eigenstrain* of the inclusion, c is the inclusion radius, ν is the Poisson ratio.

The dilatation of cylindrical inclusion Δ can also be found from Eqs. (32) with taking into account Eqs. (37)-(38):

$$\Delta^{in} = \varepsilon_{rr}^{in} + \varepsilon_{\varphi\varphi}^{in} + \varepsilon_{zz}^{in} = \frac{\partial u_r^{in}}{\partial r} + \frac{u_r^{in}}{r} + \frac{\partial u_z^{in}}{\partial z} - 3\varepsilon^* = \frac{(1+\nu)\varepsilon^*}{(1-\nu)} - 3\varepsilon^* = -\frac{2(1-2\nu)}{(1-\nu)}\varepsilon^*, \quad (40a)$$

$$\Delta^{out} = \varepsilon_{rr}^{out} + \varepsilon_{\varphi\varphi}^{out} + \varepsilon_{zz}^{out} = \frac{\partial u_r^{out}}{\partial r} + \frac{u_r^{out}}{r} + \frac{\partial u_z^{out}}{\partial z} = 0. \quad (40b)$$

It follows from Eqs. (40 a,b) that the dilatation is constant inside the inclusion and zero outside it. Analytical calculations show that hemispherical dilatational inclusion has the same dilatation [25].

The stress field can be derived by using the Hooke law for isotropic media, see Ref. [25] for details. It is easy to show that the stress fields of the axisymmetric inclusions under consideration satisfy the system of equilibrium equations [25].

The strain energy of dilatational inclusions is determined by formula [10]:

$$E = -\frac{1}{2}\int_{V_{incl}} \varepsilon_{ii}^* \sigma_{ii}^{in} dV \Rightarrow E = \frac{2G(1+\nu)\varepsilon^{*2}}{(1-\nu)} V_{incl}, \quad (41)$$

where V_{incl} is the inclusion volume.

Our direct analytical calculations demonstrated the independence of the strain energy on the shape of the inclusion with dilatational *eigenstrain*, which also confirms the correctness of the solutions found.

4. DEFECTS IN 2D CRYSTALS

Two-dimensional crystals are films whose thickness can be neglected in the problem under consideration. Among them, one can distinguish crystalline carbon films – graphenes [31,32], and carbon polyhedral shells – fullerenes [33,34]. From the point of view of continuum mechanics, such objects are 2D elastic media. A special feature of a 2D medium is its ability to have the nonzero curvature. In this way, the film reacts to external influences or to the appearance of defects in it [35-37].

We can apply the classification of defects in a 2D elastic medium based on the dimension of the region, where the self-distortions (*eigenstrains*) of the defects are specified, in the same way as it is done for defects in a 3D medium, see Part 2. According to the dimensional principle, defects in a 2D medium are subdivided into 3 types (Fig. 9).

Below, we denote the self-distortion of a defect as ${}^{m|n}\beta_{ij}^*$, where *m* is the dimension of the medium and *n* is the dimension of the defect.

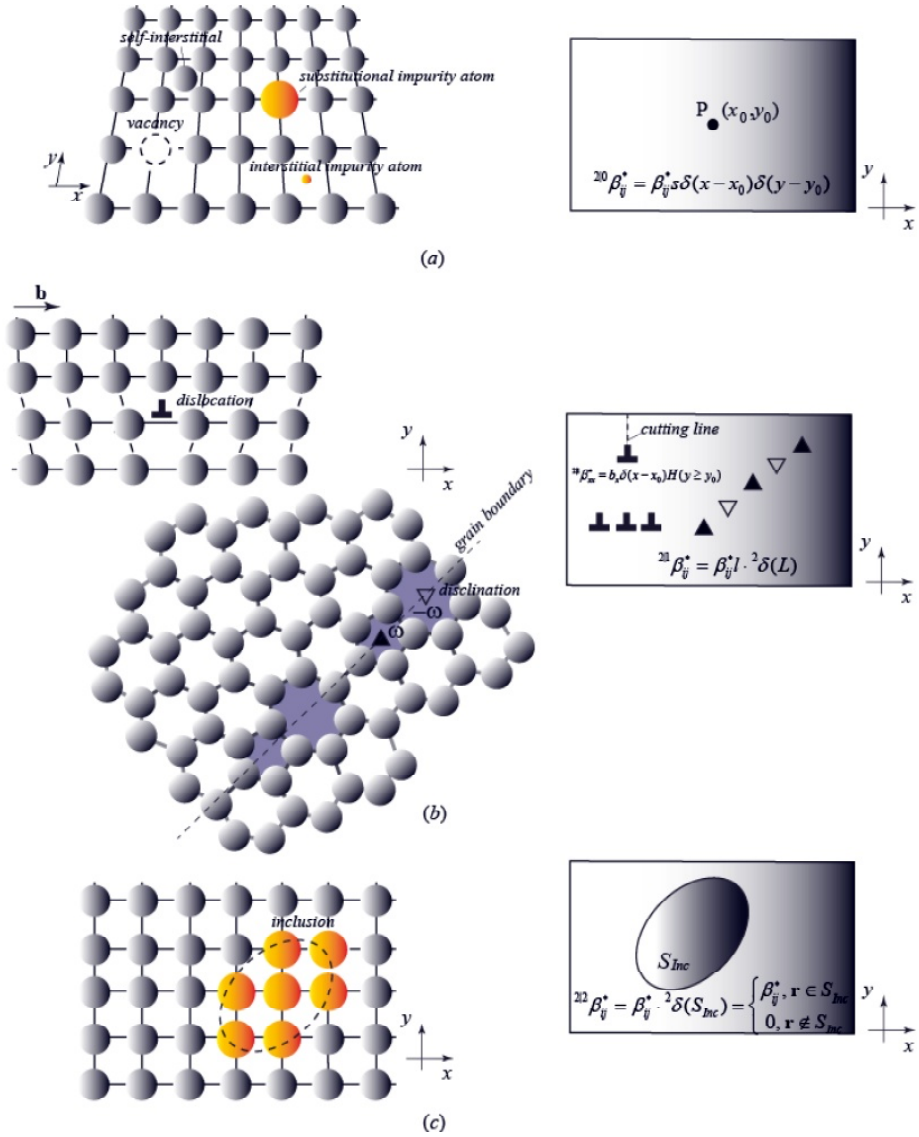

Fig. 9. Defects in 2D crystals and their elastic models. (a) Zero-dimensional defects are vacancy, self-interstitial, substitutional impurity, and interstitial impurity. (b) One-dimensional defects are dislocation, disclination, and misorientation boundary. (c) Two-dimensional inclusion. The main characteristic of a defect is its self-distortion ${}^{2|n}\beta^*_{ij}$, where n is the defect dimension and $i, j = x, y$, adapted from [38].

4.1. Classification of defects in 2D continuum

Zero-dimensional (point) defects (n=0). First, let us define an infinitesimal dislocation loop which is an elementary zero-dimensional defect in both the 2D and 3D media [38]. In the film lying in the *xy*-plane, the self-distortion of the infinitesimal dislocation loop becomes:

$$ {}^{2|0}\beta^*_{ij} = -b_j\, l_i\, \delta(\mathbf{r}-\mathbf{r}_0), \quad i, j = x, y \qquad (42)$$

where b_j is the dislocation Burgers vector; $\mathbf{r}_0$ is the coordinate of the loop on the *xy*-plane, l_i is the segment, which is an analog of the area s_i for an infinitesimal dislocation loop in the 3D medium, see Eq. (1). The two-dimensional Dirac delta function is given by the relation $\delta(\mathbf{r}-\mathbf{r}_0) = \delta(r-r_0)\delta(y-y_0)$.

Two mutually perpendicular infinitesimal dislocation loops form a dilatation center with the following distortion:

$$ {}^{2|0}\beta^*_{ii} = b\, l\, \delta(\mathbf{r}-\mathbf{r}_0) = \frac{1}{2}\Delta s\, \delta(\mathbf{r}-\mathbf{r}_0), \quad i, j = x, y, \qquad (43)$$

Such a center is an elastic model of an impurity atom or a vacancy (Fig. 9a). If l the initial linear dimension of the loop, a change in the linear dimension by an amount will lead to a change in the area by an amount. Assuming that $\Delta s=(l+\Delta l)^2-l^2 \approx 2l\Delta l$ and $b=\Delta l$, we obtain the last equality in Eq. (43).

With a formal approach, the self-distortion of a point defect in a film can be written:

$$^{2|0}\beta^*_{ij} = \beta^*_{ij}\, s\, \delta(\mathbf{r} - \mathbf{r}_0), \quad i, j = x, y, \tag{44}$$

where s is a formal dimensional factor.

One-dimensional defects (n=1). The self-distortion of a one-dimensional defect located, for example, on a segment $[y_1, y_2]$ having a coordinate x_0, reads:

$$^{2|1}\beta^*_{ij} = \beta^*_{ij}\, l\, \delta(x - x_0) H(y_1 \le y \le y_2), \tag{45}$$

where β^*_{ij} is the plastic distortion of the line segment; l is a linear factor, $H(y_1 \le y \le y_2)$ is the Heaviside function.

In the film, the Somigliana dislocations are one-dimensional defects, and the Volterra dislocations and disclinations are degenerate one-dimensional defects (Fig. 9b).

One can rewrite the distortion of the dislocation shown in Fig. 9b, to the form typical for Volterra dislocations [38]:

$$^{2|1}\beta^*_{xx} = -b_x \delta(x - x_0) H(y_0 \le y \le \infty)$$
$$\text{or} \quad ^{2|1}\beta^*_{yx} = -b_x \delta(x - x_0) H(x_0 \le x \le \infty). \tag{46}$$

A linear defect can be represented through point defects continuously distributed with some linear density along a line.

Two-dimensional defects (n=2). The area of determining the self-distortion of two-dimensional defects is a part of the surface. In a film, two-dimensional defects are similar to inclusions in a 3D medium (Fig. 9c).

For a two-dimensional defect of general form, the following expression is true:

$$^{2|2}\beta^*_{ij} = \beta^*_{ij} \begin{cases} 1, & \mathbf{r} \in S_{incl} \\ 0, & \mathbf{r} \notin S_{incl} \end{cases}. \tag{47}$$

A two-dimensional defect can also be represented through distribution of point defects over the surface S_{incl}.

It is worth noting that in a 2D continuum, defects of dimension lower than 2 are described by distortions which contain some arbitrary dimensional factors as is the case with defects of dimension lower than 3 in a 3D medium.

4.2. Elastic fields of defects in 2D planar media

In the case of 2D elastic planar medium, the self-distortion $^{2|n}\beta^*_{ij}$ (or *eigenstrain* $^{2|n}\varepsilon^*_{ij}$) allows to find, by using the Green function $^2G_{ij}$ and elastic modules C_{jlkm}, the total displacements of defects [10]:

$$^2u^t_i(\mathbf{R}) = -\int_{S'} C_{jlkm}\, {}^{2|n}\varepsilon^*_{km}(\mathbf{R}')\, {}^2G_{ij,l}(|\mathbf{r} - \mathbf{r}'|)\, \mathrm{d}S', \tag{48}$$

where the left upper index 2 indicates the dimension of the medium.

For the isotropic elastic medium, the Green function $^2G_{ij}$ and the elastic modules C_{jlkm} are [10]:

$$^2G_{ij}(|\mathbf{r} - \mathbf{r}_0|) = \frac{1}{8\pi(1-\nu)G} \times$$
$$\left\{ \frac{(x_i - x'_i)(x_j - x'_j)}{\overline{r}^2} - (3 - 4\nu)\delta_{ij} \ln \overline{r} \right\}, \tag{49a}$$

$$C_{jlkm} = \frac{2G\nu}{1-2\nu}\delta_{jl}\delta_{km} + G(\delta_{lk}\delta_{jm} + \delta_{lm}\delta_{jk}), \tag{49b}$$

where $\overline{r}^2 = (x - x')^2 + (y - y')^2$, δ_{km} is the Kronecker delta, G is the shear modulus, and ν is the Poisson ratio.

Since in our case the elastic space is a film with free surfaces, which lies in the xy-plane, the stress tensor does not contain the components σ_{zj}. This means that we deal with the plane-stress state and hence in both the Green function and Hooke law, the Young modulus E and the Poisson ratio ν should be replaced by ratios $E(1+2\nu)/(1+\nu)^2$ and $\nu/(1+\nu)$, respectively [10]. Since the shear modulus $G=E/[2(1+\nu)]$, the replacement procedure does not affect it. In the transition from the 3D case to the 2D case, the unit of measurement of the Young and shear moduli change from N/m^2 to N/m.

Using Eqs. (48) and (49), one can define the fields of an infinitesimal dislocation prismatic loop and a dilatation center.

4.2.1. Infinitesimal prismatic dislocation loop (IPDL) and dilatation center in film

The field of total displacements $^2u_i^{IPDL}(x,y)$ of an IPDL, placed in the origin of Cartesian coordinates (0, 0), is calculated from Eqs. (48) and (49) with replacement of the Poisson ratio ν by the expression $\nu/(1+\nu)$ and results in

$$^2u_x^{IPDL} = \frac{b_x l\, x}{4\pi r^4}\left[-(\nu - 1)y^2 + (3 + \nu)x^2\right], \tag{50a}$$

$$^2u_y^{IPDL} = \frac{b_x l\, x}{4\pi r^4}\left[-(\nu - 1)y^2 + (3 + \nu)x^2\right], \tag{50b}$$

where $r^2=x^2+y^2$ and b_x is the value of the IPDL Burgers vector.

The displacements (50) make it possible to find the elastic strains, and then, according to the Hooke law, the elastic stresses

$$ {}^{2}\sigma_{xx}^{IPDL} = -\frac{G(1+\nu)b_x l}{2\pi r^6}\left[3x^4 - 6x^2y^2 - y^4\right], \quad (51a)$$

$$ {}^{2}\sigma_{yy}^{IPDL} = \frac{G(1+\nu)b_x l}{2\pi r^6}\left[x^4 - 6x^2y^2 + y^4\right], \quad (51b)$$

$$ {}^{2}\sigma_{xy}^{IPDL} = -\frac{G(1+\nu)b_x l}{2\pi r^6}\left[3x^2 - y^2\right], \quad (51c)$$

Let us consider now the field of a dilatation center characterized by the self-distortion

$$ {}^{2|0}\beta_{xx}^{*\Delta P} = {}^{2|0}\beta_{yy}^{*\Delta P} = \varepsilon^* s\,\delta(x)\delta(y). \quad (52)$$

The displacement and stress fields of the dilatation center are:

$$ {}^{2}u_x^{\Delta P} = \frac{(1+\nu)\varepsilon^* s}{2\pi}\cdot\frac{x}{r^2}, \quad (53a)$$

$$ {}^{2}u_y^{\Delta P} = \frac{(1+\nu)\varepsilon^* s}{2\pi}\cdot\frac{y}{r^2}, \quad (53b)$$

$$ {}^{2}\sigma_{xx}^{\Delta P} = -\frac{G(1+\nu)\varepsilon^* s}{\pi}\cdot\frac{(x^2-y^2)}{r^4}, \quad (54a)$$

$$ {}^{2}\sigma_{yy}^{\Delta P} = \frac{G(1+\nu)\varepsilon^* s}{\pi}\cdot\frac{(x^2-y^2)}{r^4}, \quad (54b)$$

$$ {}^{2}\sigma_{zz}^{\Delta P} = -\frac{2G(1+\nu)\varepsilon^* s}{\pi}\cdot\frac{xy}{r^4}, \quad (54c)$$

$$ {}^{2}\sigma_{xx}^{\Delta P} + {}^{2}\sigma_{yy}^{\Delta P} = 0. \quad (54d)$$

The functional parts of the stress field (54) coincide with those of the stress field caused by a dilatation line in the 3D medium, see Eqs. (25).

After replacement $\varepsilon s=b_x l$ in Eqs. (53) and (54), it becomes clear that the dilatation center in the 2D medium is the sum of two mutually perpendicular IPDLs, see Eqs. (50) and (51), just as the dilatation center in the 3D medium is the sum of three mutually perpendicular IPDLs.

It is also worth to note, that the fields of a biaxial dilatation line with self-distortion in the 3D medium ${}^{3|1}\beta_{xx}^{*L} = {}^{3|1}\beta_{yy}^{*L} = \varepsilon^* s\,\delta(x)\delta(y)$ precisely coincide with fields (53) and (54) when replacing ν by $\nu/(1+\nu)$.
It is clear that defects causing a plane strain in a 3D medium have their counterparts of smaller dimension in the film. In this case, the fields of these defects in the film transform to those of their counterparts in the 3D crystal, when the elastic moduli are replaced in the appropriate way, and the condition $\sigma_{zz}=0$ is taken into account.

4.2.3. Dislocation and wedge disclination in film

Straight-line edge dislocations and wedge disclinations in 3D media generate plane strain states, see, for example, [7,39]. Therefore, the main difference between the stress fields of these defects in a film and in an infinite 3D medium is the absence of the σ_{zz} component. The other stress components of dislocations and disclinations coincide with the accuracy to the factors associated with ν.

The solutions of the boundary-value problems for edge dislocations and wedge disclinations perpendicular to the free surfaces of a plate having a finite thickness, are presented in [11,40]. In particular, it was shown in [41] that when the plate thickness tends to zero, the elastic field generated by the edge dislocation becomes as that in the plane stress state.

Notice that the disclination dipole is a characteristic element of grain boundaries in graphene (Fig. 9b), see, for example, [36,37]. Using the rows of disclination dipoles with their elastic fields, it was possible to calculate the strain energy of grain boundaries in graphene without exploiting the computer simulation [41].

4.2.4. Dilatation inclusion in the film

An example of a dilatation inclusion in a 2D medium is shown in Fig. 9c. On the base of the stresses of a biaxial cylindrical inclusion in a 3D medium having eigenstrain

$$ {}^{3}\varepsilon_{xx}^{*} = {}^{3}\varepsilon_{yy}^{*} = \begin{cases}\varepsilon^*, \boldsymbol{R} \in \Omega_{incl} \\ 0, \boldsymbol{R} \in \Omega_{incl}\end{cases}, $$

the stresses of circular dilatational inclusion in 2D crystal with eigenstrain

$$ {}^{2|2}\varepsilon_{xx}^{*} = {}^{2|2}\varepsilon_{yy}^{*} = \begin{cases}\varepsilon^*, \boldsymbol{r} \in S_{incl} \\ 0, \boldsymbol{r} \in S_{incl}\end{cases}, $$

can be written, replacing ν by $\nu/(1+\nu)$ and neglecting σ_{zz} [21]:

$$^{2}\sigma_{xx}^{incl} = G(1+\nu)\varepsilon^{*}a^{2}\begin{cases} -\dfrac{(x^{2}-y^{2})}{r^{4}}, r > a \\ \dfrac{2}{a^{2}}, r \le a \end{cases}, \qquad (55a)$$

$$^{2}\sigma_{yy}^{incl} = G(1+\nu)\varepsilon^{*}a^{2}\begin{cases} \dfrac{(x^{2}-y^{2})}{r^{4}}, r > a \\ \dfrac{2}{a^{2}}, r \le a \end{cases}, \qquad (55b)$$

$$^{2}\sigma_{zz}^{incl} = G(1+\nu)\varepsilon^{*}a^{2}\begin{cases} -\dfrac{2xy}{r^{4}}, r > a \\ 0, r \le a \end{cases}, \qquad (55c)$$

Here *a* is a radius of the inclusion

If we introduce the radius of the core for the biaxial dilatation center *a* and determine the coefficient *s* in Eq. (54) as πa^2, then the stresses of dilatation center are coincide with the stresses generated by the circular biaxial inclusion in the surrounding matrix *r>a* (55).

5. SUMMARY AND CONCLUSIONS

Classification of defects of an elastic continuum, presented in the paper, is based on the dimension of the region, where the self-distortion or *eigenstrain* of the defect is localized. It allows to determine the place of structural defects – inclusions, dislocations and disclinations – in the hierarchy of defects of the elastic continuum. For example, if the scale parameters of the elastic problem are much larger than the size of the defect, one can operate with point or one-dimensional defects.

We have discussed how to create defects of higher dimension from defects of smaller dimension. On the base of the elastic fields of the infinitesimal dislocation loops, the fields of the circular dilatation line, the circular dilatation disk, and finite cylindrical and hemispherical inclusions are derived in a step-by-step manner.

We have also presented the elastic models of defects in flat 2D crystals. Using the self-distortion, the elastic fields of an infinitesimal dislocation loop and a dilatational center in the film are calculated. It is shown that the defects creating a plane-strain state in a 3D elastic medium have their counterparts in a 2D medium.

If to consider the theory of defects wider, we can extend it beyond the framework of the elastic field and apply it to the fields of different physical nature: electromagnetic and gravitational. Based on the known field equations with a known Green function and specifying a counterpart of the *eigenstrain*, for example, the density of electric charge and the density of mass, etc., it is possible to calculate the fields of defects of any dimension and, in particular, to take into account the time coordinate. The formalized approach allows not only to calculate the fields of defects, but also makes it possible to find parallels in the behavior of defects of different nature.

ACKNOWLEDGEMENTS

Authors thank the Ministry of Education and Science of the Russian Federation for its support (Project No 3.3194.2017/4.6).

REFERENCES

[1] V. Volterra // *Annales Scientifique de l'École Normale Supérieure. Paris* **24 (4)** (1907) 401.
[2] J.D. Eshelby // *Proceedings of the Royal Society of London A* **241** (1957) 376.
[3] J.D. Eshelby, *Continual Theory of Dislocations* (Publisher of Foreign Literature, Moscow, 1963), In Russian.
[4] *Collected Works of J.D. Eshelby. The Mechanics of Defects and Inhomogeneties*, ed. by Xanthippi Markenscoff and Anurag Gupta (Springer, Notherlands, 2006).
[5] F. Kroupa, In: *Theory of Crystal Defects*. Proceedings of the Summer School held in Hrazany in September 1964 (Academia - Publishing House of the Czechoslovak Academy of Sciences, Prague, 1966), p. 276.
[6] V.L. Indenbom, In: *Theory of Crystal Defects*. Proceedings of the Summer School held in Hrazany in September 1964 (Academia - Publishing House of the Czechoslovak Academy of Sciences, Prague, 1966), p. 257.
[7] R. De Wit, *Continual Theory of Disclinations* (Mir, Moscow, 1977), In Russian.
[8] J.P. Hirth and J. Lothe, *Theory of dislocations* (John Wiley and Sons, New York/ Chichester/ Brisbane/ Toronto/ Singapore, 1982).
[9] C. Teodosiu, *Elastic Models of Crystal Defects* (Springer-Verlag, 1982).
[10] T. Mura, *Micromechanics of Defects in Solids* (Martinus Nijhoff Publishers, Dordrecht/ Boston/Lancaster, 1987).
[11] A.L. Kolesnikova and A.E. Romanov, *Circular dislocation-disclination loops and their*

application to boundary problem solution in the theory of defects (Phys.-Tech. Inst., Preprint No 1019, Leningrad, 1986), In Russian.
[12] A.Yu. Belov, In: *Elastic Strain Fields and Dislocation Mobility*, ed. by V.L. Indenbom and J. Lothe (Elsevier, 1992).
[13] A.L. Kolesnikova and A.E. Romanov // *Journal of Applied Mechanics* **71 (3)** (2004) 409.
[14] N. Louat // *Nature (London)* **196 (4859)** (1962) 1081.
[15] M.J. Marcinkowski, *Unified Theory of the Mechanical Behavior of Matter* (John Wiley and Sons, New York, 1979).
[16] A.M. Korsunsky // *Journal of Elasticity* **44** (1996) 97.
[17] R.J.H. Paynter, D.A. Hills and A.M. Korsunsky // *International Journal of Solids and Structures* **44** (2007) 6653.
[18] Yu.N. Rabotnov, *Mechanics of the Deformed Solids* (Nauka, Moscow, 1979), In Russian.
[19] R.J. Asaro and V.A. Lubarda, *Mechanics of Solids and Materials* (Cambridge University Press, New York, 2006).
[20] P.P. Groves and D.J. Bacon // *Journal of Applied Physics* **40** (1969) 4207.
[21] A.L. Kolesnikova, R.M. Soroka and A.E. Romanov // *Materials Physics and Mechanics* **17(1)** (2013) 71.
[22] T. Mura, In: *Advanced in Materials Research*, ed. by H. Herman (Interscience Publ., New York, 1968), Vol. 3, p. 1.
[23] T. Mura // *Archives of Mechanics* **24 (3)** (1972) 449.
[24] A. Howie and L.D. Marks // *Philosophical Magazine A* **49** (1984) 95.
[25] A.L. Kolesnikova, M.Yu. Gutkin and A.E. Romanov // *International Journal of Solids and Structures* (2017) (submitted).
[26] A.M. Campbell and J. Evetts, *Critical Currents in Superconductors* (Taylor & Francis Ltd, United Kingdom, 1972).
[27] M.Yu. Gutkin and I.A. Ovid'ko // *The European Physical Journal B* **1(4)** (1998) 429.
[28] E. Jahnke, F Emde and F. Losch, *Tafeln höherer Funktionen* (Stuttgart, Teubner, 1960).
[29] G. Eason, B. Noble and I.N. Sneddon // *Philosophical Transactions of the Royal Society of London* **247 (935)** (1955) 529.
[30] A.I. Lur'e, *Spatial Problems of Theory of Elasticity* (State Publishing House of Scientific and Technical Literature, Moscow, 1955), In Russian.
[31] K.S. Novoselov, D. Jiang, F. Schedin, T.J. Booth, V.V. Khotkevich, S.V. Morozov and A.K. Geim // *Proceedings of the National Academy of Sciences of the United States of America* **102** (2005) 10451.
[32] M.I. Katsnelson, *Graphene: Carbon in Two Dimensions* (New York: Cambridge University Press, 2012).
[33] H.W. Kroto, J.R. Heath, S.C. O'Brien, R.F. Curl and R.E. Smalley // *Nature* **318** (1985) 162.
[34] J. Baggott, *Perfect Symmetry: The Accidental Discovery of Buckminsterfullerene* (Oxford University Press, 1995).
[35] A.L. Kolesnikova and A.E. Romanov // *Physics of the Solid State* **40(6)** (1998) 1075.
[36] B.I. Yakobson and F. Ding // *ACS NANO* **5** (2011) 1569.
[37] J. Zhang and J. Zhao // *Carbon* **55** (2013) 151.
[38] A.L. Kolesnikova, T.S. Orlova, I. Hussainova and A.E. Romanov // *Physics of the Solid State* **56(12)** (2014).
[39] A.E. Romanov and V.I. Vladimirov, *In: Dislocations in Solids,* ed. by F.R.N. Nabarro (North-Holland, Amsterdam, 1992), Vol. 9, p. 191.
[40] A.L. Kolesnikova and A.E. Romanov // *Technical Physics Letters* **3(6)** (1987) 272.
[41] A.E. Romanov, A.L. Kolesnikova, T.S. Orlova, I. Hussainova, V.E. Bougrov and R.Z. Valiev // *Carbon* **81(1)** (2015) 223.